Supplementary Information

Probing the active sites of Co_3O_4 for acidic oxygen evolution reaction by modulating Co^{2+}/Co^{3+} ratio

Kai-Li Yan [a], Jun-Feng Qin [a], Jia-Hui Lin [a, b], Bin Dong [*a, b], Jing-Qi Chi [a], Zi-Zhang Liu [a, b], Fang-Na Dai [a, b], Yong-Ming Chai [*a], Chen-Guang Liu [a]

a State Key Laboratory of Heavy Oil Processing, China University of Petroleum (East China), Qingdao 266580, PR China

b College of Science, China University of Petroleum (East China), Qingdao 266580, PR China

~~Synthesis process of Ag-~~Co_3O_4'

* Corresponding author. Email: dongbin@upc.edu.cn (B. Dong), ymchai@upc.edu.cn (Y.M. Chai)

Tel: +86-532-86981376, Fax: +86-532-86981787

2.1811 g $Co(NO_3)_2.6H_2O$, 0.45 g urea are completely dissolved in 35 mL deionized water, then the mixture is transferred into a 100-mL Teflon lined stainless steel autoclave. After keep a constant temperature of 120°C for 6 h, the resulting precipitate was collected and washed with deionized water and alcohol, and then calcinated at

400°C for 2 h in air to obtain Co_3O_4'. The as-prepared Co_3O_4' of 0.1 g is further dissolved in 0.08 M CTAB. At the same time, 0.016 M $AgNO_3$ is subsequently added into the aboved solution, followed by the addition of 0.2 M ascorbic acid solutions. The resultant solution is maintained at 60°C for 4 hours. After washed with deionized water and alcohol, the Ag-Co_3O_4' is obtained.

Calculation of mass activity (j_m, A g^{-1})

The mass activity, j_m, is calculated by eq (1) [1] :

$$j_m = j_{geo}/m \quad (1)$$

where j_{geo} is the measured current density per geometric area (mA cm_{geo}^{-2}) at a given overpotential, m is the catalyst loading 0.2 (mg cm_{geo}^{-2}).

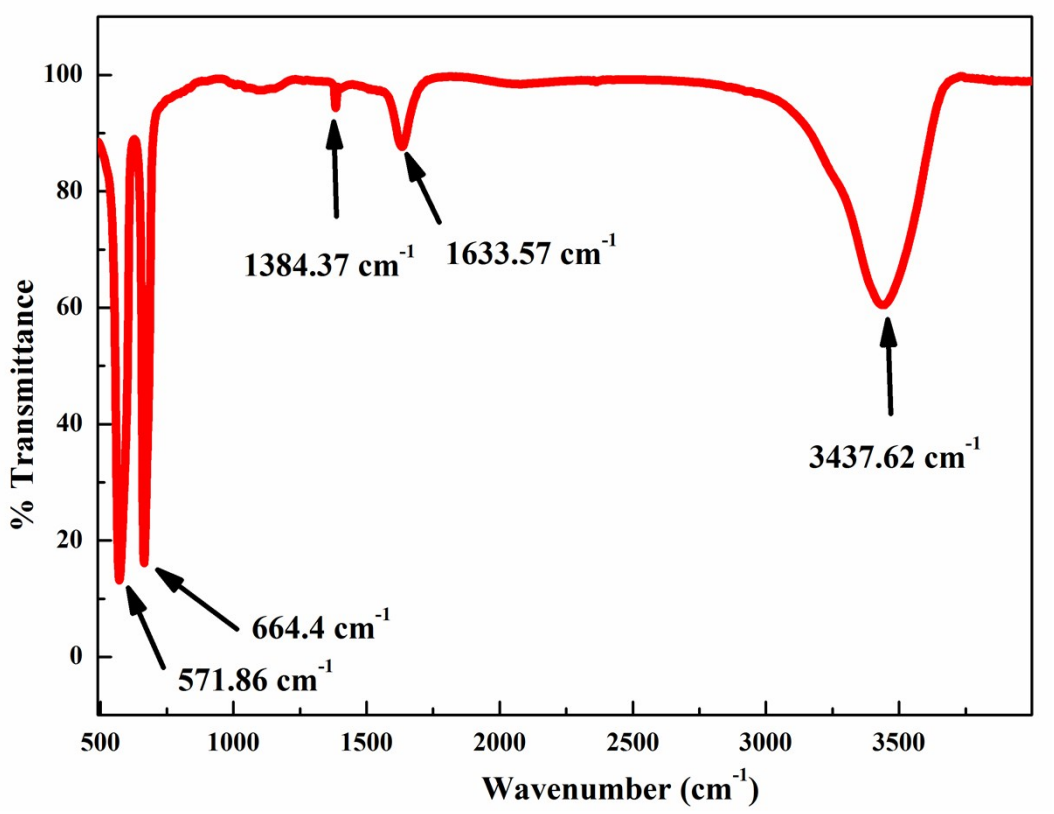

Fig. S1 FT-IR of Ag-Co_3O_4 (400).

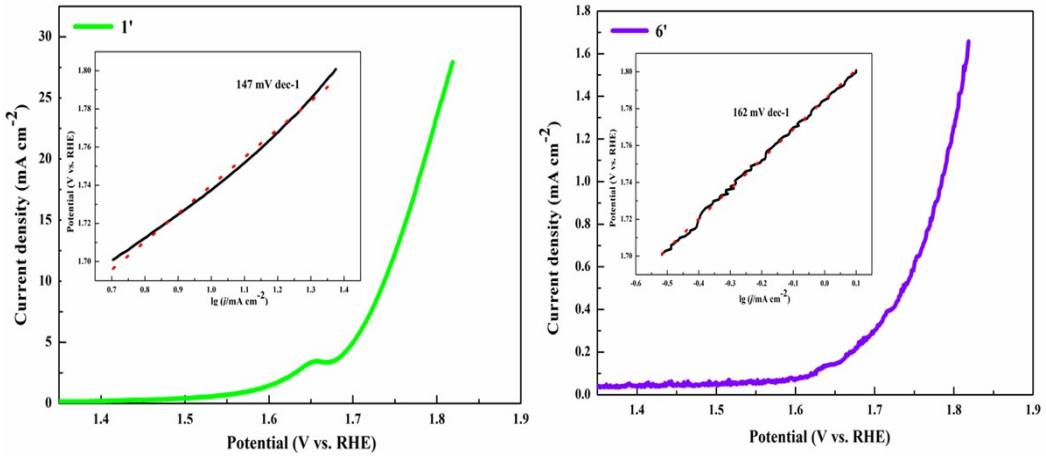

(a) Ag-Co_3O_4-1

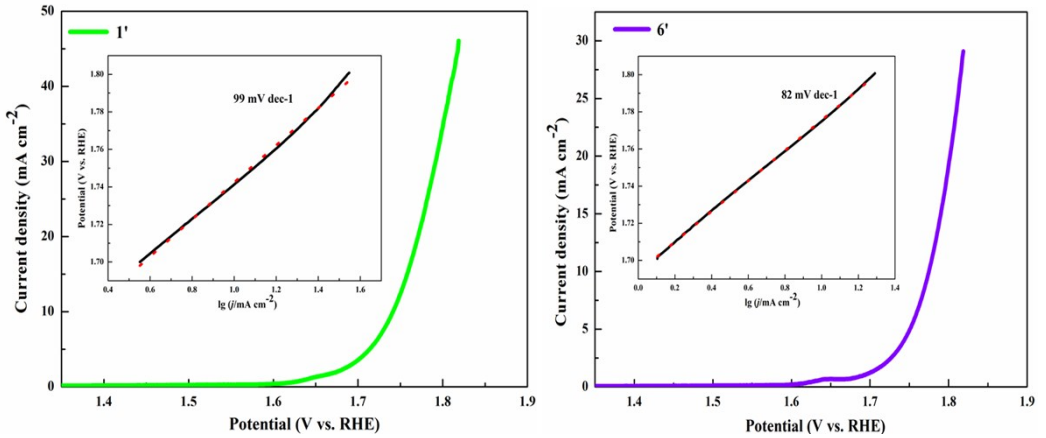

(b) Ag-Co_3O_4-2

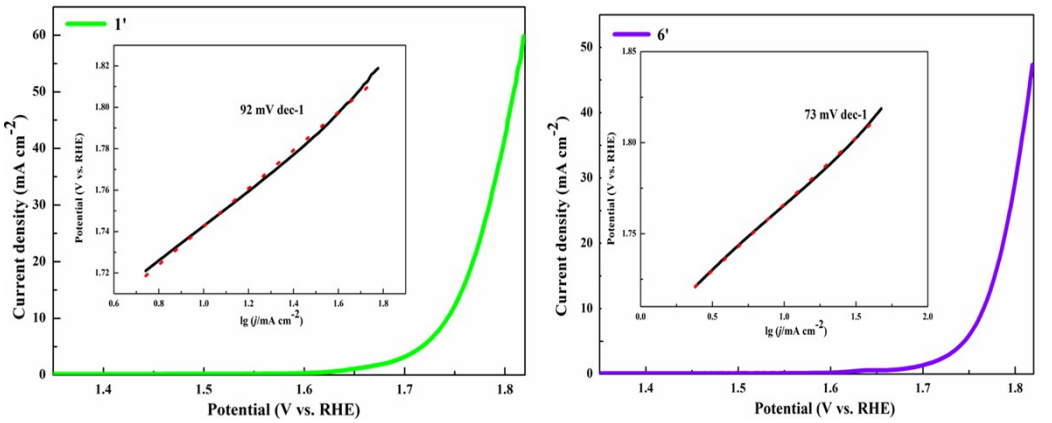

(c) Ag-Co_3O_4-3

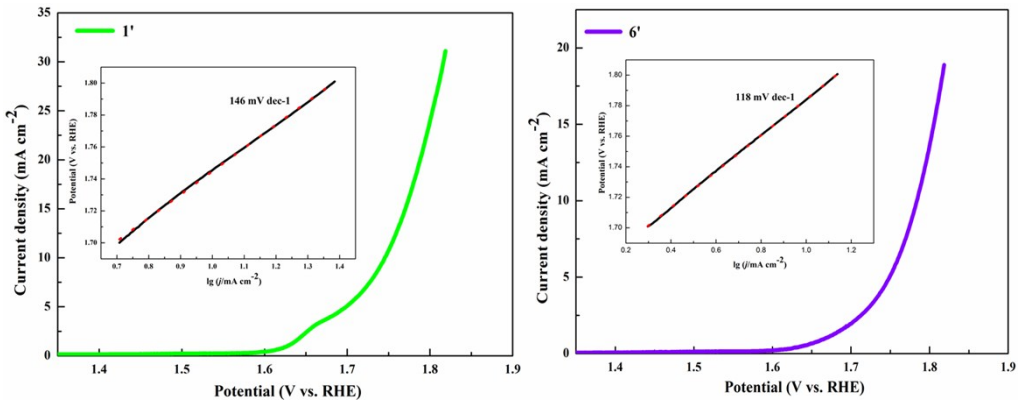

(d) Ag-Co_3O_4-4

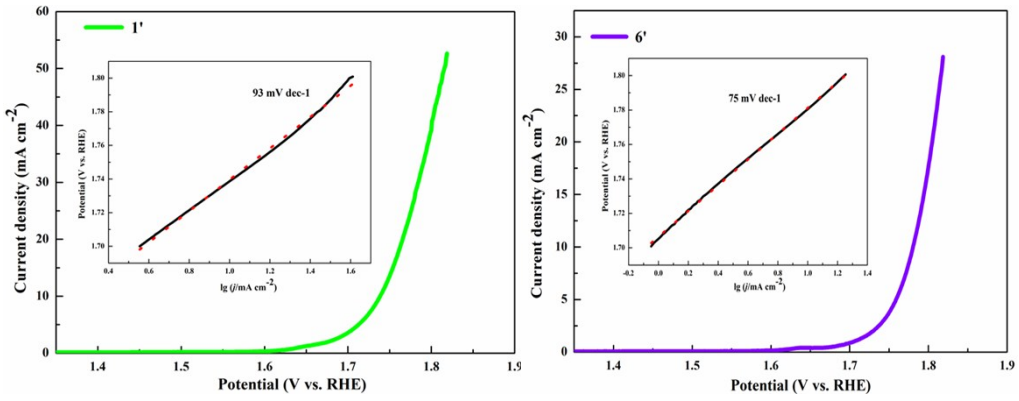

(e) Co_3O_4-5

Fig. S2 Polarization curves (inset image is corresponding Tafel slopes) measured with Ag-Co_3O_4 samples in 0.5 M H_2SO_4 electrolyte. wherein the Ag-Co_3O_4-1, Ag-Co_3O_4-2, Ag-Co_3O_4-3, Ag-Co_3O_4-4 and Co_3O_4-5 represents the precursor ratio of $AgNO_3/Co(NO_3)_2.6H_2O$= 0.1/2.4, 0.05/2.45, 0.025/2.475, 0.0125/2.4825 and 0/2.5, respectively. It concludes that the Ag-Co_3O_4-3 sample (denote as Ag-Co_3O_4 for brevity in the main text) exhibited the best OER activities.

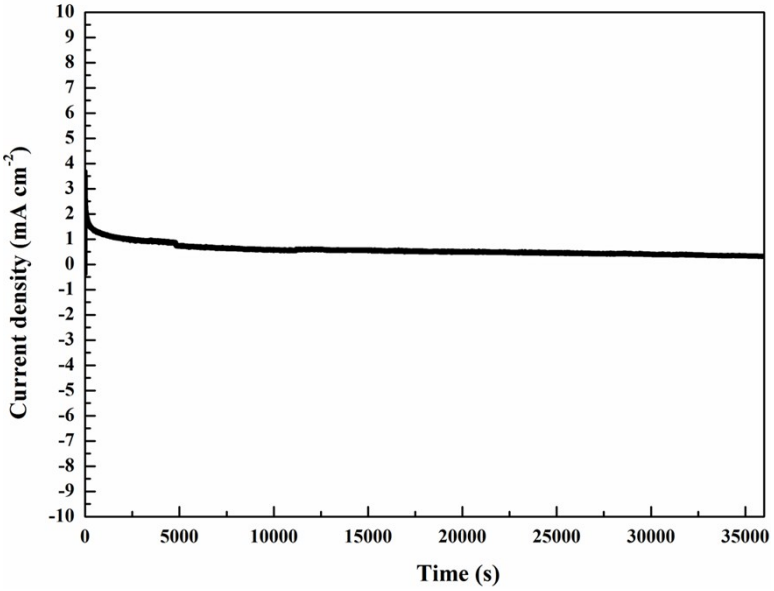

Fig. S3 Chronoamperometry curve of the Ag-Co_3O_4 (400) at 1.72 V vs. RHE.

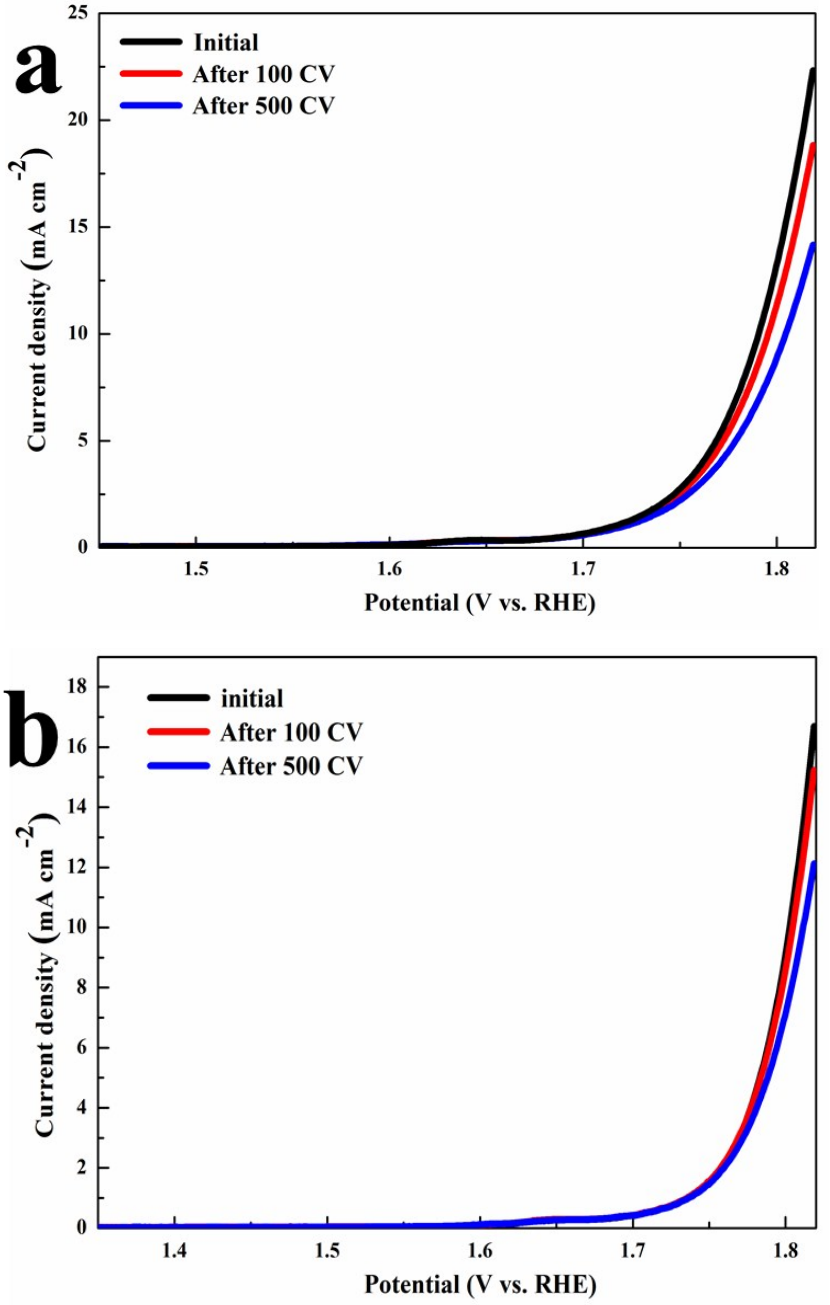

Fig. S4 Plot of current density vs. potential for (a) Ag-Co_3O_4-500 and (b) Ag-Co_3O_4-600 electrodes in 0.5 M H_2SO_4 initially (black) and also after 100 (red) and 500 (blue) CV sweeps between 1.66 and 1.76 V vs. RHE at a scan rate of 100 mV s^{-1}.

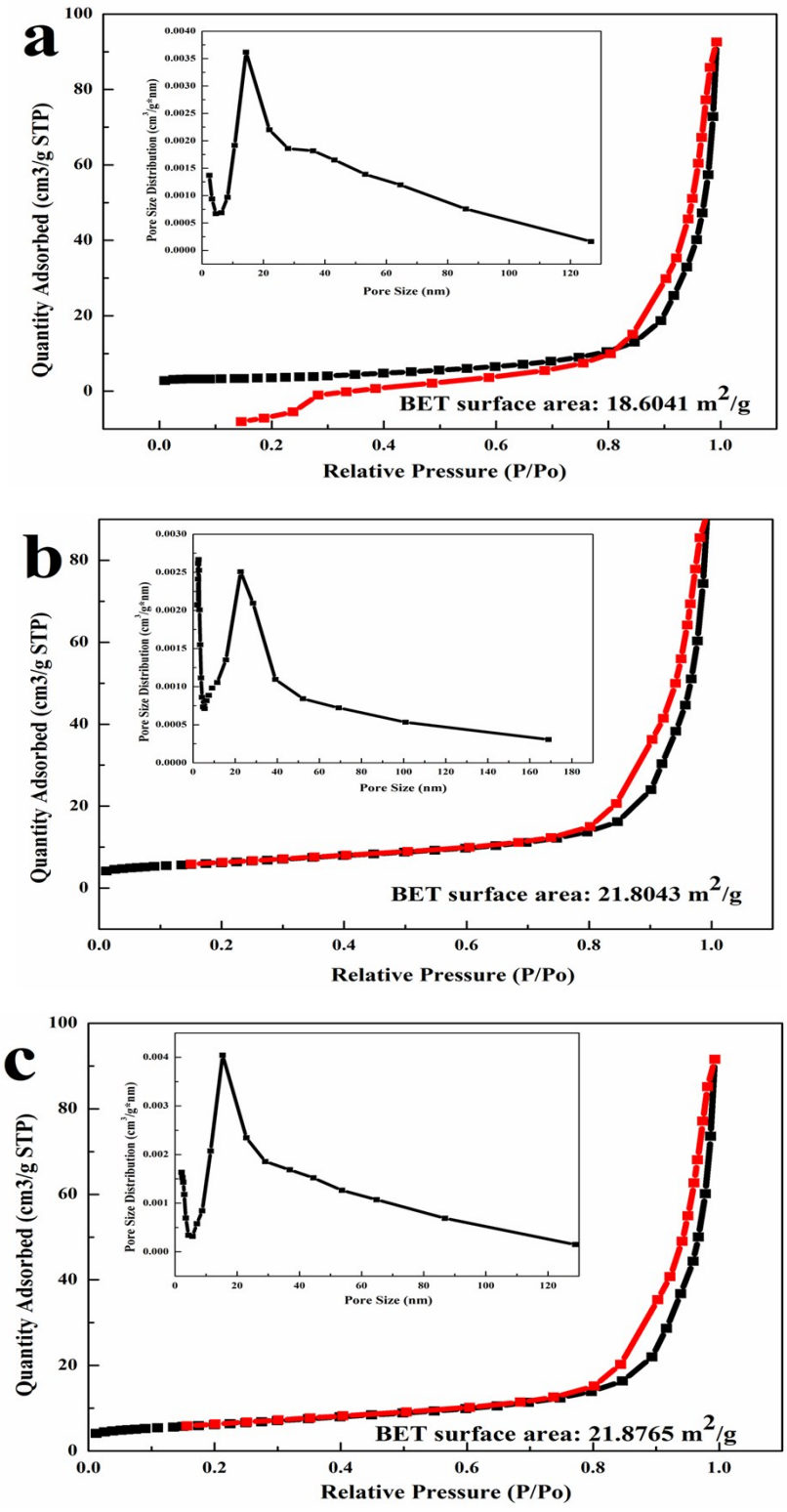

Fig. S5 N_2 adsorption isotherms of Ag-Co_3O_4 samples (inset: pore size distribution):

(a) Ag-Co_3O_4 (400) (b) Ag-Co_3O_4 (500) (c) Ag-Co_3O_4 (600).

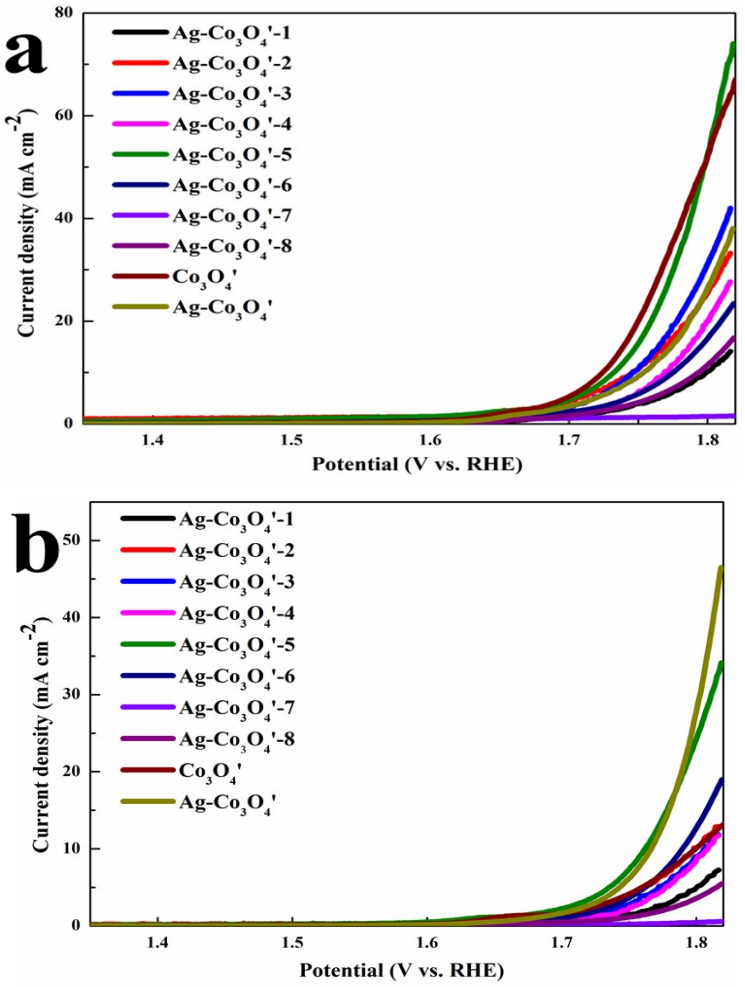

Fig. S6 (a) The first and (b) The tenth polarization curves measured with Ag-Co_3O_4' samples in 0.5 M H_2SO_4 electrolyte. wherein the Ag-Co_3O_4'-1 represents the $AgNO_3$ and ascorbic acid is 0.032 M and 0.4 M, respectively. Ag-Co_3O_4'-2 represents the $AgNO_3$ and ascorbic acid is 0.008 M and 0.1 M, respectively. Ag-Co_3O_4'-3 and Ag-Co_3O_4'-4 represents the CTAB is 0.04 and 0.16 M, respectively. Ag-Co_3O_4'-5 and Ag-Co_3O_4'-6 represents the CTAB is replaced by PVP and SDS, respectively. Ag-Co_3O_4'-7 and Ag-Co_3O_4'-8 represents the reduction time is 2 and 8 h, respectively. It concludes that the Ag-Co_3O_4' sample exhibited the best OER activities.

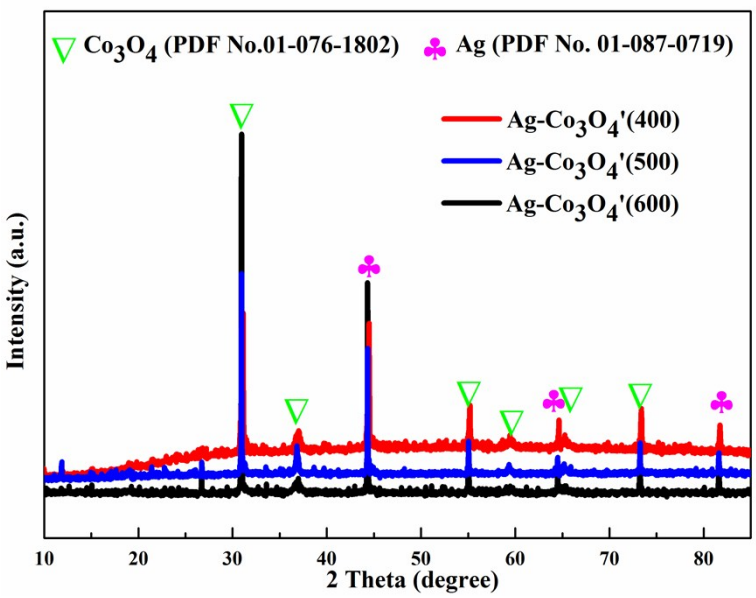

Fig. S7 XRD patterns of Ag-Co_3O_4' (400), Ag-Co_3O_4' (500) and Ag-Co_3O_4' (600)

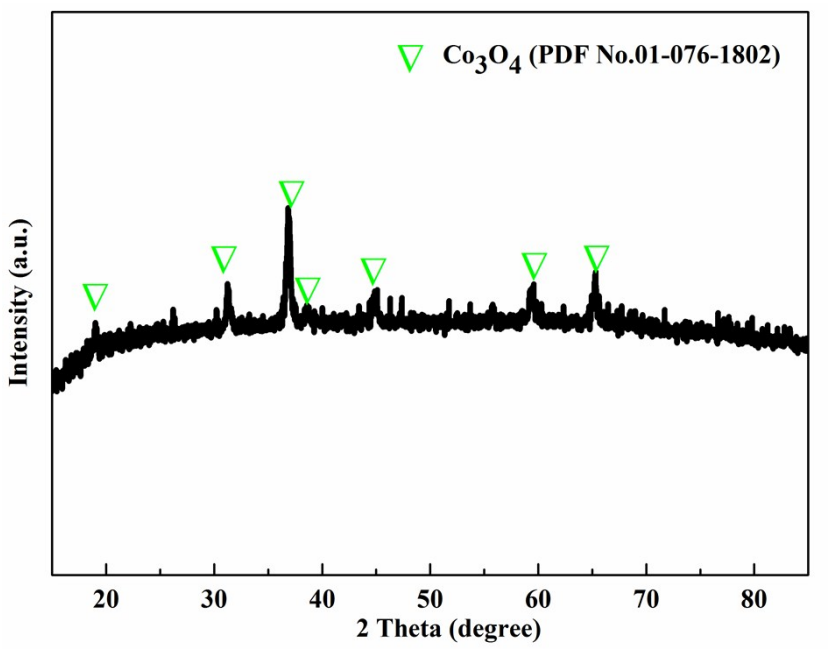

Fig. S8 XRD pattern of Co_3O_4'

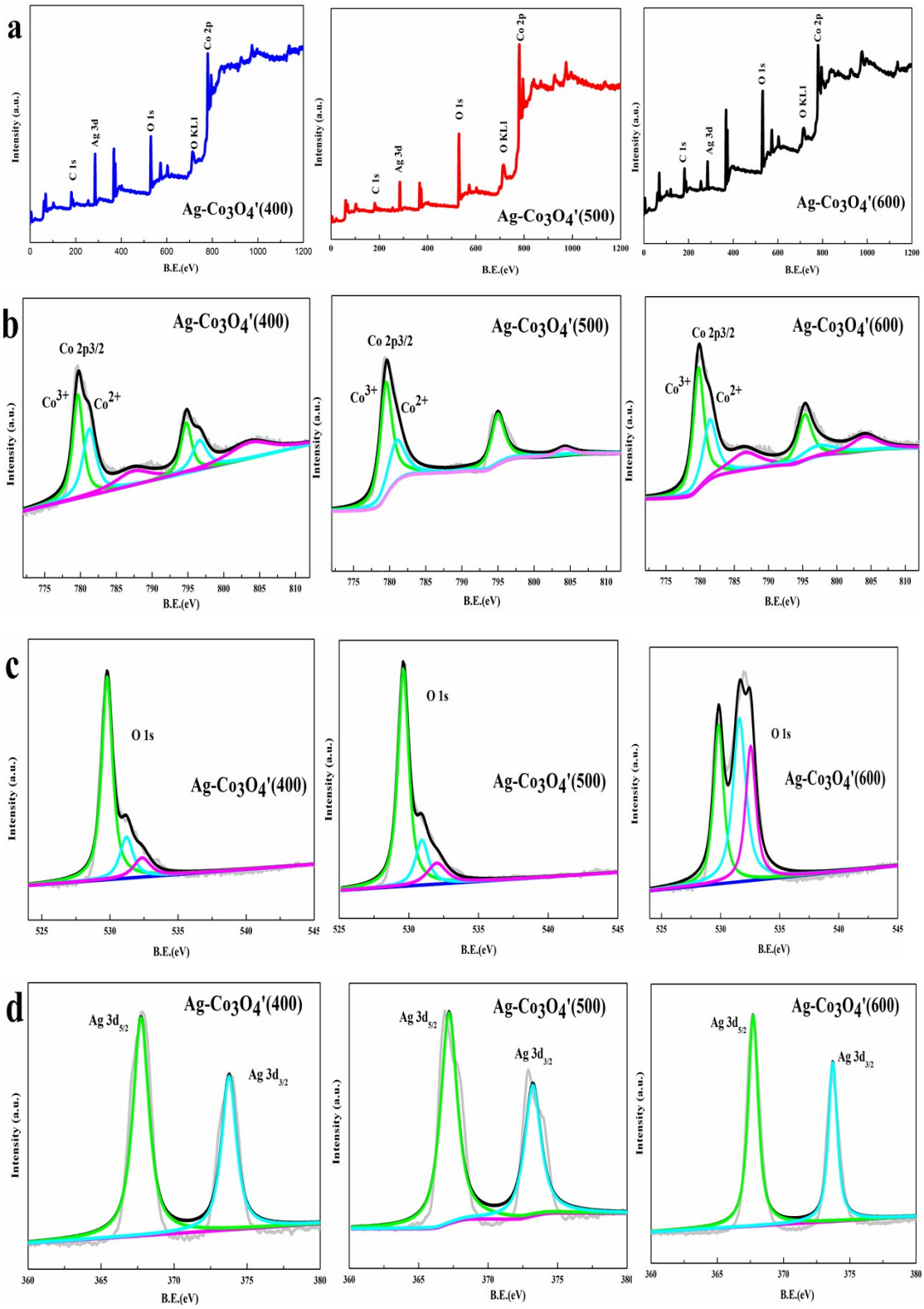

Fig. S9 XPS spectra of (a) survey (b) Co 2p (c) O 1s and (d) Ag 3d for Ag-Co_3O_4' (400), Ag-Co_3O_4' (500) and Ag-Co_3O_4' (600)

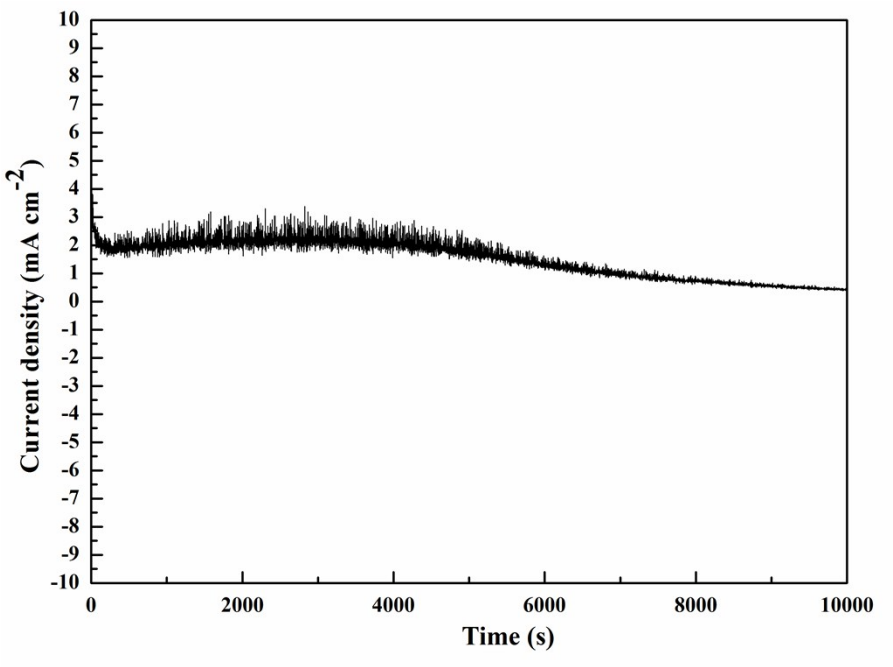

Fig. S10 Chronoamperometry curve of the Ag-Co_3O_4' (400) at 1.72 V vs. RHE.

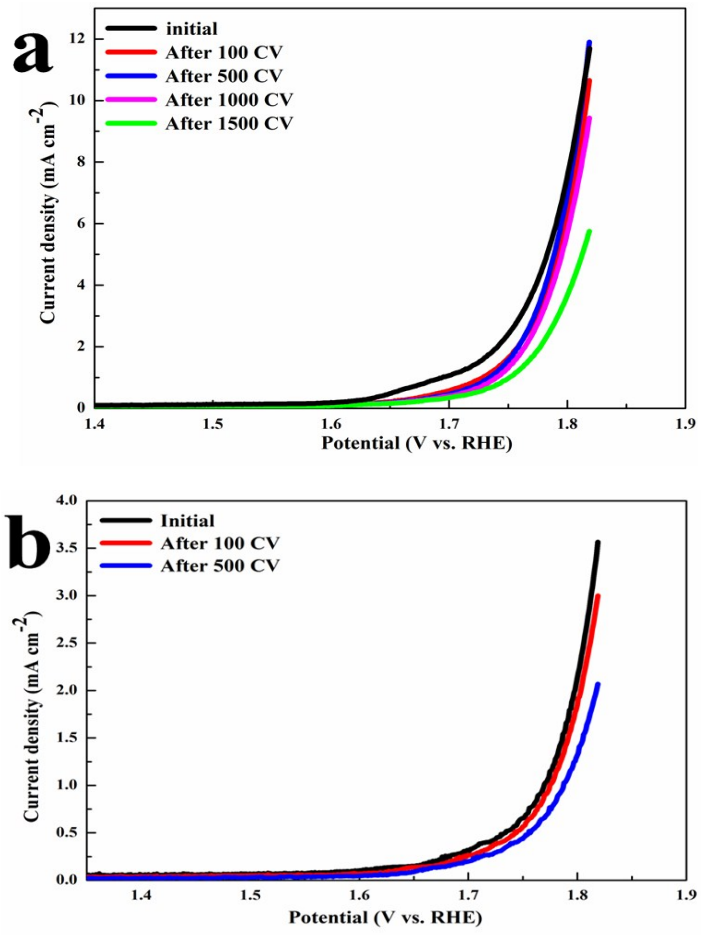

Fig. S11 Plot of current density vs. potential for (a) Ag-Co_3O_4'-500 and (b) Ag-Co_3O_4'-600 electrodes in 0.5 M H_2SO_4 initially (black) and also after 100 (red) and 500 (blue) and 1000 (purple) and 1500 (green) CV sweeps between 1.66 and 1.76 V vs. RHE at a scan rate of 100 mV s^{-1}.

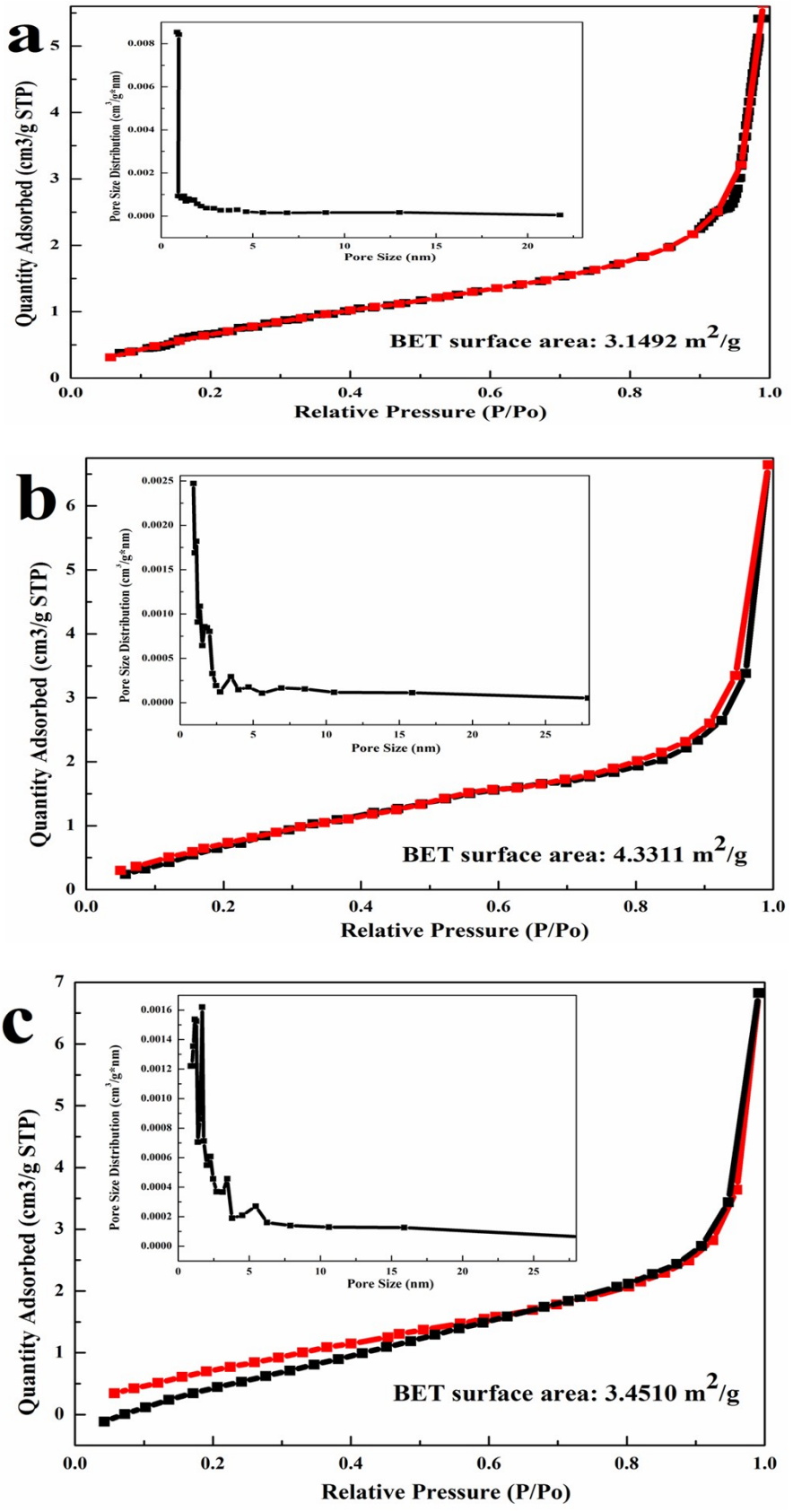

Fig. S12 N_2 adsorption isotherms of Ag-Co_3O_4' samples (inset: pore size distribution):

(a) Ag-Co_3O_4'(400) (b) Ag-Co_3O_4'(500) (c) Ag-Co_3O_4'(600)

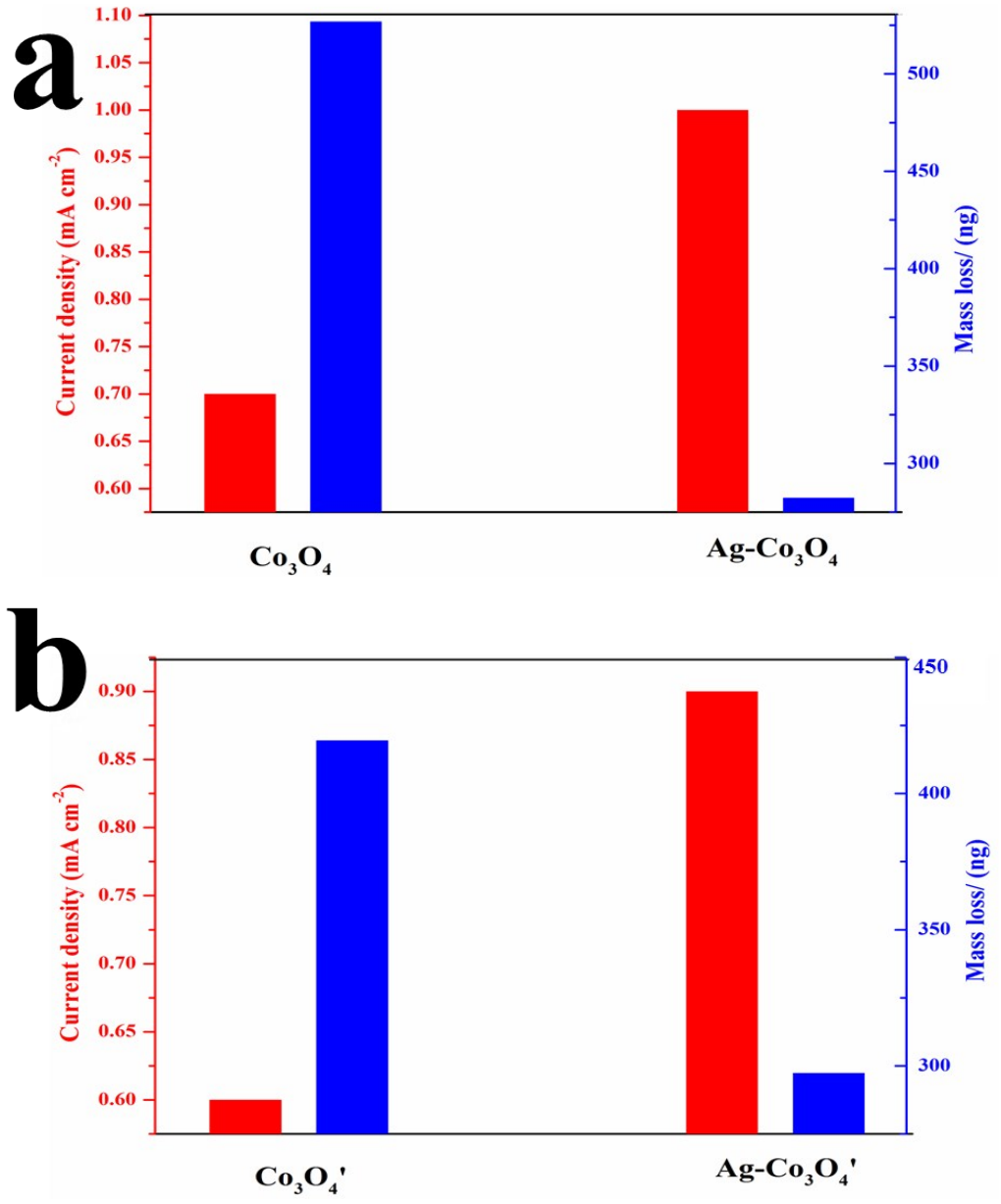

Fig. S13 Acidic OER activity and Mass loss of Co after 2 h chronoamperometry tests at 1.72 V vs. RHE: (a) Ag-Co_3O_4 sample (b) Ag-Co_3O_4' sample

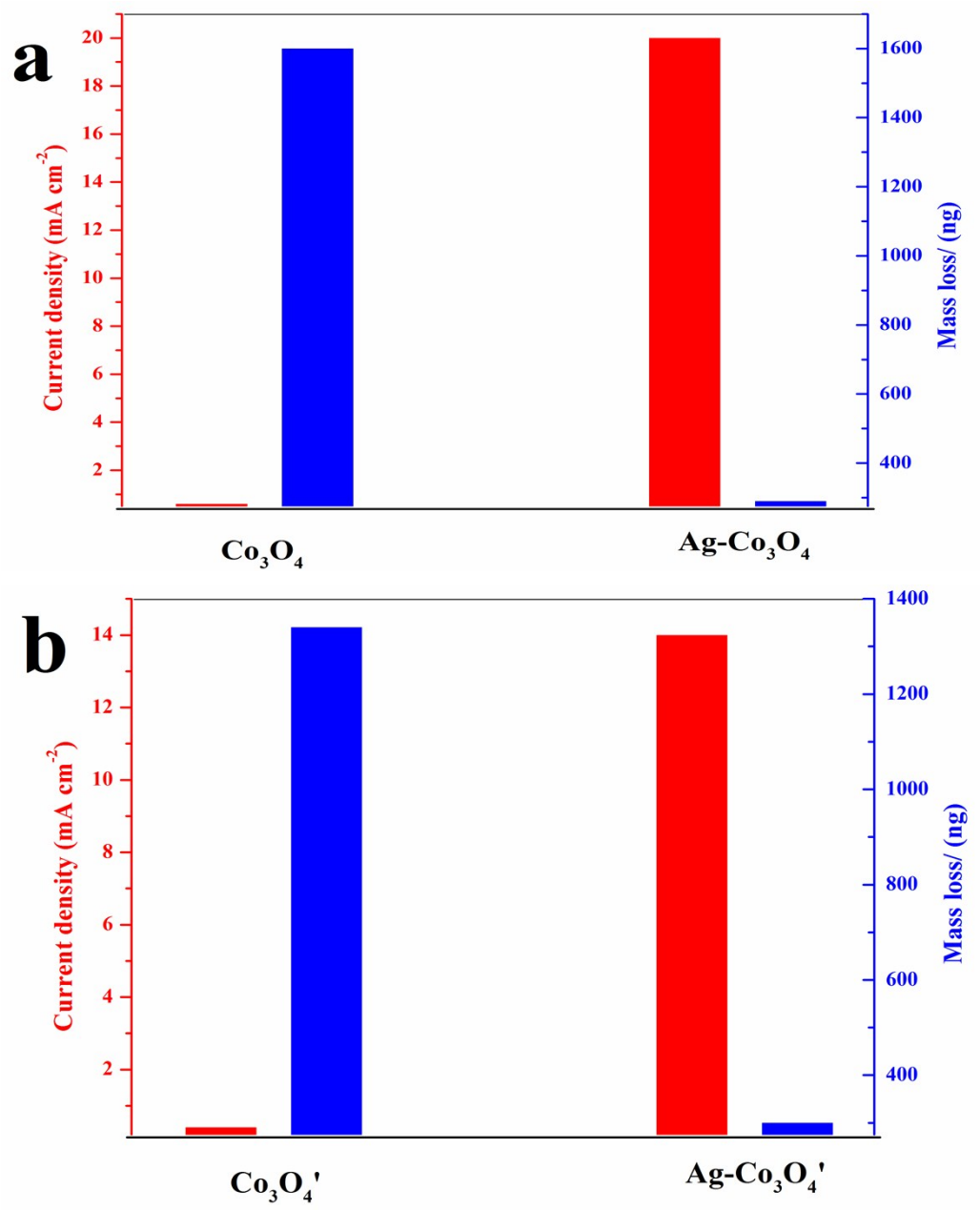

Fig. S14 Acidic OER activity and Mass loss of Co after 2 h chronoamperometry tests at 1.82 V vs. RHE: (a) Ag-Co_3O_4 sample (b) Ag-Co_3O_4' sample.

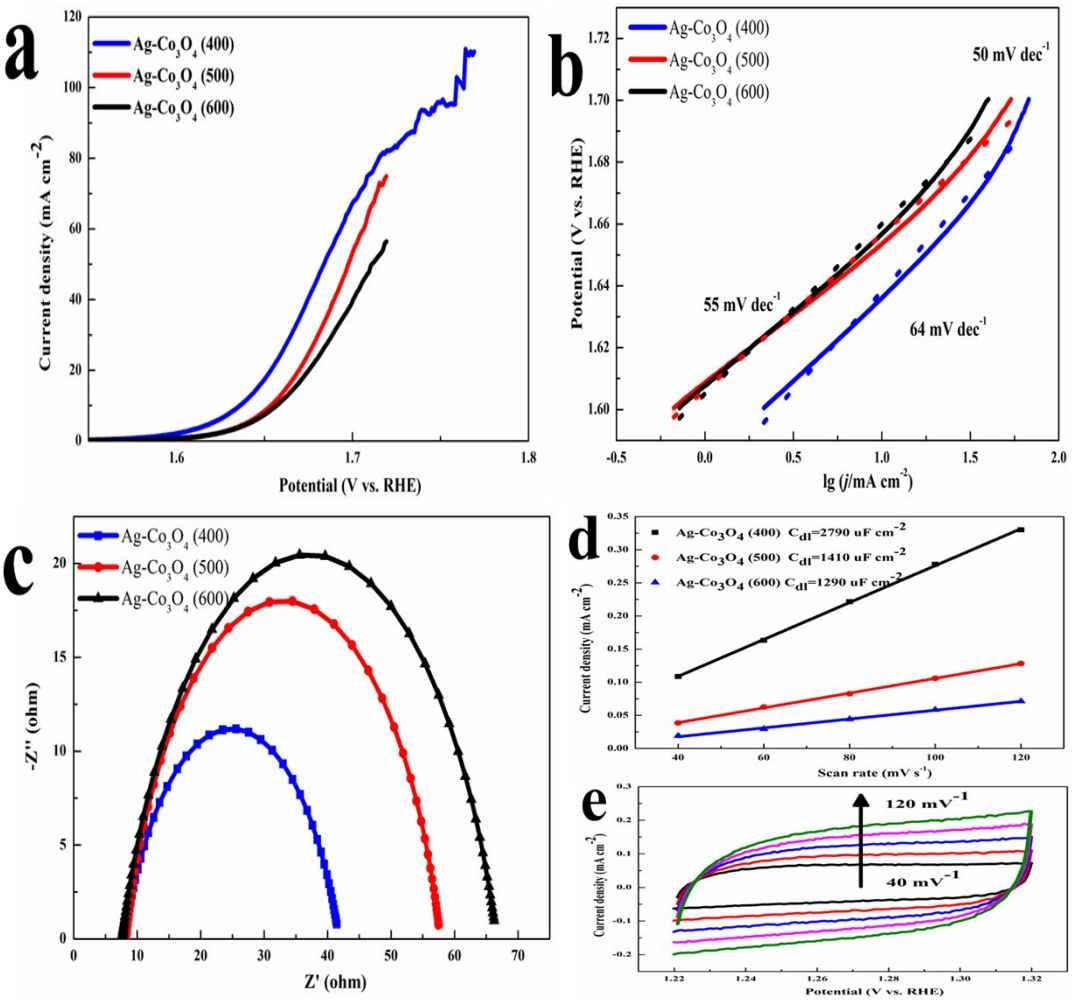

Fig. S15 OER activity of Ag-Co_3O_4 measured in 1 M KOH. (a) The OER polarization curves (b) The corresponding Tafel slopes. (c) Nyquist plots. (d) Liner fitting of the current density vs. the scan rate at 1.27 V vs. RHE. (e) Cyclic voltammograms of Ag-Co_3O_4 (400) at scan rates from 40 to 120 mV s^{-1}.

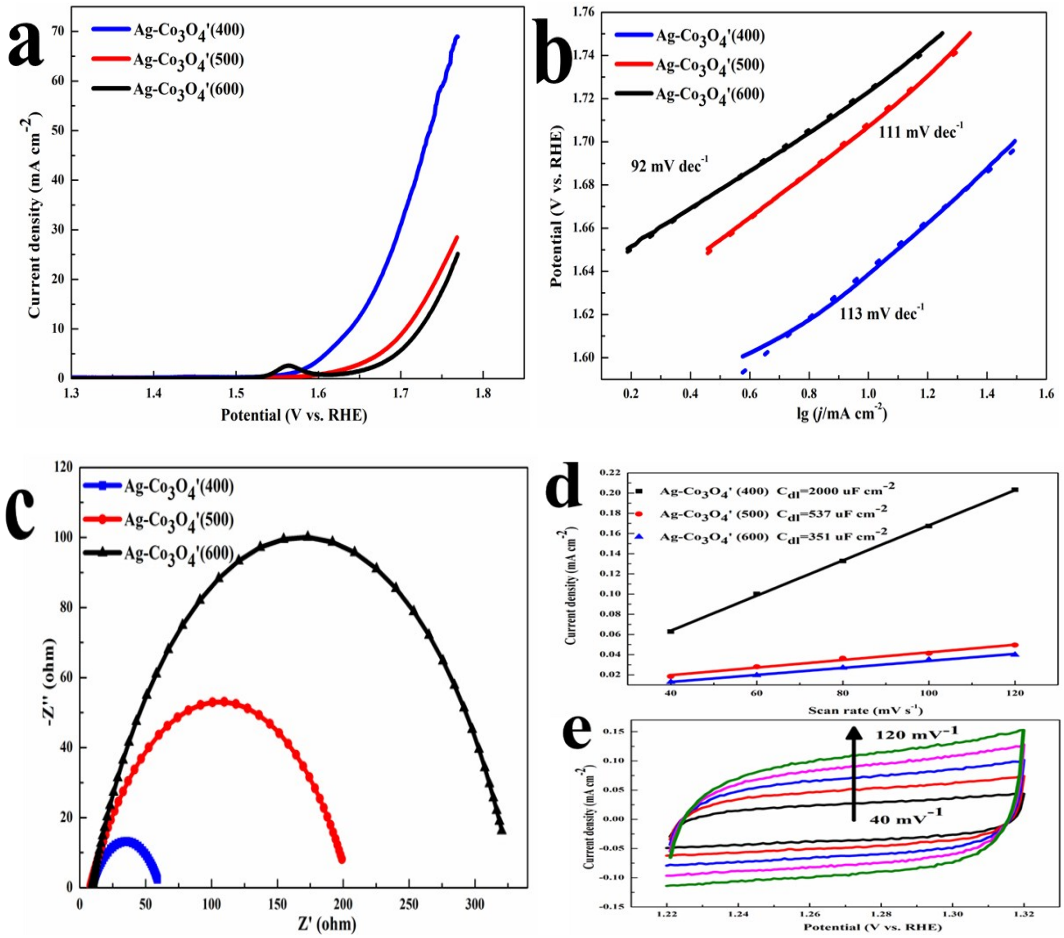

Fig. S16 OER activity of Ag-Co_3O_4' measured in 1 M KOH. (a) The OER polarization curves (b) The corresponding Tafel slopes. (c) Nyquist plots. (d) Liner fitting of the current density vs. the scan rate at 1.27 V vs. RHE. (e) Cyclic voltammograms of Ag-Co_3O_4' (400) at scan rates from 40 to 120 mV s^{-1}.

Table S1 Comparison of the OER activity of the Ag-Co_3O_4 with other nonprecious electrocatalysts in acidic media.

Catalysts	**Overpotential/mV (J=10mAcm^{-2})**	**Electrolyte**	**Ref.**
Ag-Co_3O_4	**470**	**0.5 M H_2SO_4**	**This work**
Crystalline Cobalt Oxide Films	570	0.5 M H_2SO_4	2
Ti-MnO_2	_	0.05 M H_2SO_4	3
$Ni_{0.5}Mn_{0.5}Sb_{1.7}Oy$	672 ±9	1 M H_2SO_4	4
NiFeP	540	0.05 M H_2SO_4	5

Table S2 The atomic ratio of Co^{2+}/Co^{3+} derived from XPS results for the Ag-Co_3O_4 (400), Ag-Co_3O_4 (500) and Ag-Co_3O_4 (600).

Catalysts	**Atomic ratio of Co^{2+}/Co^{3+}**	**Fitted area of Co^{2+}(Co^{3+})**
Ag-Co_3O_4 (400)	**0.62**	**40364.7**
		(65104.3)
Ag-Co_3O_4 (500)	0.53	81840.84
		(154416.67)
Ag-Co_3O_4 (600)	0.4	16843.22
		(42108.05)

Table S3 Comparison of the acidic OER activity of the Ag-Co_3O_4 with different ratio of $AgNO_3/Co(NO_3)_2.6H_2O$ in precursor.

Catalyst	***J*/mA cm^{-2} at 1. 8 V (vs. RHE) after 1' LSV**	***J*/mA cm^{-2} at 1. 8V (vs. RHE) after 6' LSV**	***J*/mA cm^{-2} at 1. 8 V (vs. RHE) after 10' LSV**
Ag-Co_3O_4-1 (Ag/Co=0.1/2.4)	23.74	1.26	0.66
Ag-Co_3O_4-2 (Ag/Co=0.05/2.45)	35.26	19.5	13.65
Ag-Co_3O_4-3 (Ag/Co=0.025/2.475)	**42.57**	**30.06**	**24.39**
Ag-Co_3O_4-4 (Ag/Co=0.0125/2.4825)	24.23	13.77	12.12
Co_3O_4-5 (Ag/Co=0/2.5)	19.71	17.94	13.56

Table S4 Comparison of acidic OER parameters for Ag-Co_3O_4 sample.

Catalyst	$J_{m,\eta=0.57\ V}$/A g^{-1}	BET/m^2 g^{-1}	$J_{m,\eta}$/BET	Rct/Ω	Rct/BET
Ag-Co_3O_4 (400)	216	18.6041	11.61	130	6.99
Ag-Co_3O_4 (500)	144	21.8043	6.60	160	7.34
Ag-Co_3O_4 (600)	80	21.8765	3.66	325	14.86

Table S5 Comparison of the OER activity of the Ag-Co_3O_4' under different synthesis process.

Catalyst	***J*/mA cm^{-2} at 1. 8 V (vs. RHE) after 1' LSV**	***J*/mA cm^{-2} at 1. 8V (vs. RHE) after 6' LSV**
Ag-Co_3O_4'-1	10.2	5.1
Ag-Co_3O_4'-2	25.8	10.2
Ag-Co_3O_4'-3	31.4	9.0
Ag-Co_3O_4'-4	20.0	8.7
Ag-Co_3O_4'-5	53.1	24.4
Ag-Co_3O_4'-6	17.0	12.9
Ag-Co_3O_4'-7	1.4	0.4
Ag-Co_3O_4'-8	11.7	3.6
Co_3O_4'	55.5	10.1
Ag-Co3O4'	**26.6**	**28.0**

Table S6 The ratio of Co^{2+}/Co^{3+} derived from XPS results for the Ag-Co_3O_4' (400), Ag-Co_3O_4' (500) and Ag-Co_3O_4'(600).

Catalysts	**Atomic ratio of Co^{2+}/Co^{3+}**	**Fitted area of Co^{2+}(Co^{3+})**
Ag-Co_3O_4' (400)	0.83	13469.88 (16228.8)
Ag-Co_3O_4' (500)	0.51	39554.13 (77557.1)
Ag-Co_3O_4' (600)	0.5	14998.68 (29997.36)

Table S7 Comparison of acidic OER parameters for Ag-Co_3O_4' sample.

Catalyst	$J_{m,\eta=0.57\ V}$/A g^{-1}	BET/m^2 g^{-1}	$J_{m,\eta}$/BET	Rct/Ω	Rct/BET
Ag-Co_3O_4' (400)	136	3.1492	43.18	345	109.56
Ag-Co_3O_4' (500)	40	4.3311	9.23	645	148.92
Ag-Co_3O_4' (600)	20	3.4510	5.79	815	236.16

Table S8 Normalized current density for Ag-Co_3O_4-400, Ag-Co_3O_4-500 and Ag-Co_3O_4-600 in 1 M KOH.

Catalyst	***J*/mA cm^{-2} at 1. 65 V (vs. RHE)**	**Cdl/uF cm^{-2}**	**Normalization (*J*/Cdl)**
Ag-Co_3O_4 (400)	18	2790	0.00645
Ag-Co_3O_4 (500)	9	1410	0.00638
Ag-Co_3O_4 (600)	8	1290	0.00620

Table S9 Normalized current density for Ag-Co_3O_4'-400, Ag-Co_3O_4'-500 and Ag-Co_3O_4'-600 in 1 M KOH.

Catalyst	***J*/mA cm^{-2} at 1. 65 V (vs. RHE)**	**Cdl/uF cm^{-2}**	**Normalization (*J*/Cdl)**
Ag-Co_3O_4' (400)	12.6	2000	0.0063
Ag-Co_3O_4' (500)	2.9	537	0.0054
Ag-Co_3O_4' (600)	1.5	351	0.0043

Table S10 Comparison of basic OER parameters for Ag-Co_3O_4 sample.

Catalyst	$J_{m,\eta=0.47\ V}$/A g^{-1}	$J_{m,\eta}$/BET	C_{dl}/BET	Rct/BET
Ag-Co_3O_4 (400)	338.2	18.18	149.97	2.26
Ag-Co_3O_4 (500)	268.85	12.33	64.67	2.61
Ag-Co_3O_4 (600)	200.1	9.15	58.97	3.11

Table S11 Comparison of basic OER parameters for Ag-Co_3O_4' sample.

Catalyst	$J_{m,\eta=0.47\ V}$/A g^{-1}	$J_{m,\eta}$/BET	C_{dl}/BET	Rct/BET
Ag-Co_3O_4' (400)	155.85	49.49	635.08	20.32
Ag-Co_3O_4' (500)	44.35	10.24	123.99	46.18
Ag-Co_3O_4' (600)	28.75	8.33	101.71	94.18

References

1 L. Zhuang, L. Ge, Y. Yang, M. Li, Y. Jia, X. Yao, Z. Zhu, *Adv. Mater.* 2017, **29**, 1606793.

2 J.S. Mondschein, J.F. Callejas, C.G. Read, J.Y.C. Chen, C.F. Holder, C.K. Badding, and R.E. Schaak, *Chem. Mater.*, 2017, **29**, 950.

3 R. Frydendal, E.A. Paoli, I. Chorkendorff, J. Rossmeisl and I.E.L. Stephens, *Adv. Energy Mater.*, 2015, **5**, 1500991.

4 I.A. Moreno-Hernandez, C.A. MacFarland, C.G. Read, K.M. Papadantonakis, B.S. Brunschwig and N.S. Lewis, *Energy Environ. Sci*, 2017, **10**, 2103.

5 F. Hu, S. Zhu, S. Chen, Y. Li, L. Ma, T. Wu, Y. Zhang, C. Wang, C. Liu, X. Yang, L. Song, X. Yang and Y. Xiong, *Adv. Mater.*, 2017, **29**, 1606570.